Figure 1

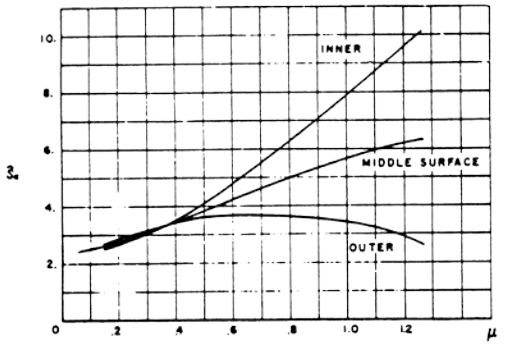

A—$\hat{S}_\epsilon$ for $\phi = 0$ vs. $\beta\rho_0$ (capped cylinder), $\nu = 0.3$

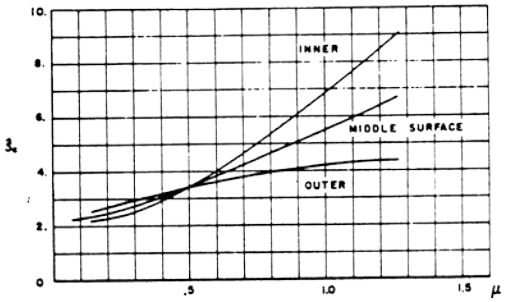

B—$\hat{S}_\epsilon$ for $\phi = \pi/8$ vs. $\beta\rho_0$ (capped cylinder), $\nu = 0.3$

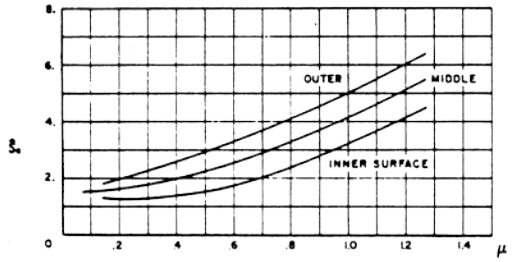

C—$\hat{S}_\epsilon$ for $\phi = \pi/4$ vs. $\beta\rho_0$ (capped cylinder), $\nu = 0.3$

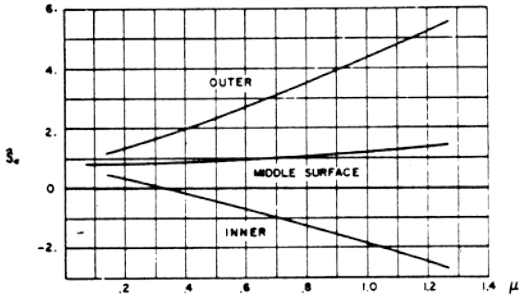

D—$\hat{S}_\epsilon$ for $\phi = 3\pi/8$ vs. $\beta\rho_0$ (capped cylinder), $\nu = 0.3$

NOTE
REFERENCE: "STATE OF STRESS IN A CIRCULAR CYLINDRICAL SHELL WITH A CIRCULAR HOLE," WELDING RESEARCH COUNCIL BULLETIN 102, 1965.

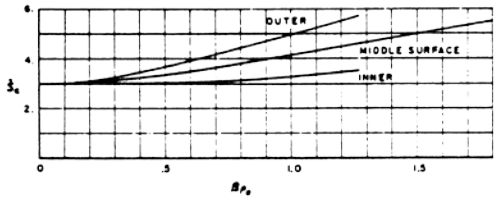

F—$\hat{S}_\epsilon$ at $\phi = \pi/2$ for Case II (extension case) vs. $\beta\rho_0$, $\nu = 0.3$

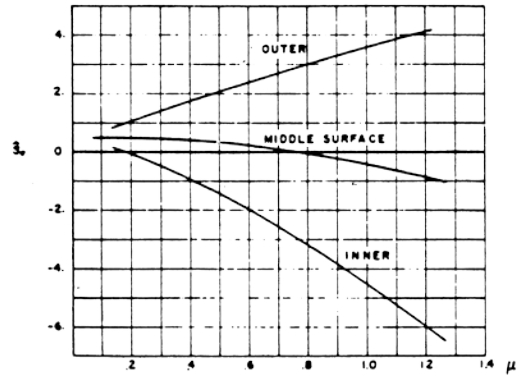

E—$\hat{S}_\epsilon$ for $\phi = \pi/2$ vs. $\beta\rho_0$ (capped cylinder), $\nu = 0.3$

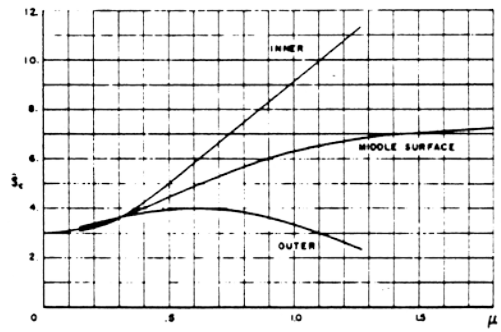

G—$\hat{S}_\epsilon$ at $\phi = 0$ for Case III (internal pressure), $\nu = 0.3$

GILBERT ASSOCIATES, INC.

FIGURE 1

Figure 2

Table 3—Stress Concentration Factor Variations for Different $\beta\rho_0$ at Various Angles—Capped Cylinder

$r = 0.30$

$\beta\rho_0$	$(\hat{S}_c)upper$	S_c	$(\hat{S}_c)lower$
	$\phi = 0$		
0.14142	2.75054	2.64709	2.54365
0.21213	2.94174	2.81900	2.69625
0.28284	3.13290	3.03670	2.94050
0.35355	3.30842	3.28570	3.26297
0.42426	3.45933	3.55467	3.65001
0.49497	3.58032	3.83486	4.08940
0.56568	3.66795	4.11911	4.57027
0.63639	3.72044	4.40201	5.08357
0.70710	3.73656	4.67874	5.62091
0.84852	3.66013	5.20121	6.74228
0.98994	3.44158	5.66463	7.88769
1.13137	3.09080	6.05690	9.02300
1.27279	2.61996	6.37120	10.12243
	$\phi = \pi/8$		
0.14142	2.46986	2.33179	2.19372
0.21213	2.66925	2.47978	2.29030
0.28284	2.87265	2.67011	2.46758
0.35355	3.06813	2.89212	2.71611
0.42426	3.25013	3.13783	3.02553
0.49497	3.41623	3.40126	3.38629
0.56568	3.56589	3.67806	3.79024
0.63639	3.69959	3.96509	4.23059
0.70710	3.81810	4.25958	4.70107
0.84852	4.01561	4.86482	5.71403
0.98994	4.16952	5.48212	6.79472
1.13137	4.29120	6.10374	7.91627
1.27279	4.39120	6.72431	9.05741
	$\phi = \pi/4$		
0.14142	1.79394	1.56884	1.34374
0.21213	2.01190	1.65385	1.29580
0.28284	2.23906	1.76710	1.29514
0.35355	2.46809	1.90438	1.33966
0.42426	2.70142	2.06304	1.42466
0.49497	2.93776	2.24160	1.54544
0.56568	3.18071	2.43944	1.69816
0.63639	3.43312	2.65648	1.87983
0.70710	3.69754	2.89277	2.08800
0.84852	4.27107	3.42439	2.57771
0.98994	4.91382	4.03512	3.15642
1.13137	5.63074	4.72359	3.81643
1.27279	6.42060	5.48575	4.55090
	$\phi = 3\pi/8$		
0.14142	1.12040	0.80340	0.48640
0.21213	1.35527	0.81807	0.28087
0.28284	1.59750	0.83819	0.07888
0.35355	1.84227	0.86252	−0.11723
0.42426	2.08946	0.88996	−0.30954
0.49497	2.34032	0.91983	−0.50065
0.56568	2.59629	0.95182	−0.69263
0.63639	2.85862	0.98593	−0.88675
0.70710	3.12823	1.02243	−1.08337
0.84852	3.69078	1.10414	−1.48249
0.98994	4.28578	1.20142	−1.88293
1.13137	4.91210	1.31959	−2.27291
1.27279	5.56731	1.46418	−2.63894
	$\phi = \pi/2$		
0.21213	1.08342	0.46892	−0.14557
0.28284	1.32929	0.44570	−0.43787
0.35355	1.57420	0.41483	−0.74454
0.42426	1.81691	0.37473	−1.06744
0.49497	2.05720	0.32403	−1.40912
0.56568	2.29480	0.26158	−1.77164
0.63639	2.52926	0.18654	−2.15617
0.70710	2.75997	0.09861	−2.56273
0.84852	3.20626	−0.11635	−3.43897
0.98994	3.62829	−0.38079	−4.38988
1.13137	4.02201	−0.68968	−5.40137
1.27279	4.38777	−1.03524	−6.45827

Table 3-Continued

$\beta\rho_0$	$\hat{S}_c$ (*Middle Surface only*) $\phi = 0$	$\pi/10$	$\pi/5$	$3\pi/10$	$2\pi/5$	$\pi/2$
1.4142	6.6163	7.1556	7.2307	4.7269	0.6424	−1.4030
1.5909	6.7936	7.7349	8.3542	5.6384	0.6623	−1.8994
1.7677	6.9059	8.4207	9.5285	6.6467	0.7164	−2.4293

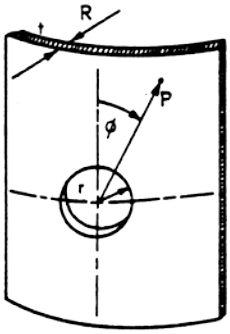

$$\mu = \frac{1}{2}\sqrt[4]{3\,(1-\nu^2)}\;\frac{r}{\sqrt{Rt}}$$

The membrane stress concentration factor S_c and the total stress concentration factor $\hat{S}_c$ are, respectively, defined by

$$S_c = \frac{\text{largest of } (N_1, N_2)}{\text{largest of } (N_1^0, N_2^0)} = \hat{S}_c \qquad \text{(middle surface)}$$

$$\hat{S}_c = \frac{\text{largest of } (\sigma 1, \sigma 2)}{\text{largest of } (\sigma 1^0, \sigma 2^0)} \quad \text{(for fixed } r, \phi)$$

where N_1^0, N_2^0 are the nominal principal stress resultants and $\sigma 1^0$, $\sigma 2^0$ are the nominal flexural stresses for the shell under the same loading but without the hole. N_1 and N_2 denote the principal stress resultants, σ_1 and σ_2 the principal stresses respectively. The stress concentration factor is calculated as a function of ϕ.

NOTE
REFERENCE: "STATE OF STRESS IN A CIRCULAR CYLINDRICAL SHELL WITH A CIRCULAR HOLE," WELDING RESEARCH COUNCIL BULLETIN 102, 1965.

GILBERT ASSOCIATES, INC.

FIGURE 2

Figure 3

STRESS DISTRIBUTION AROUND OPENINGS IN CYLINDRICAL SHELLS

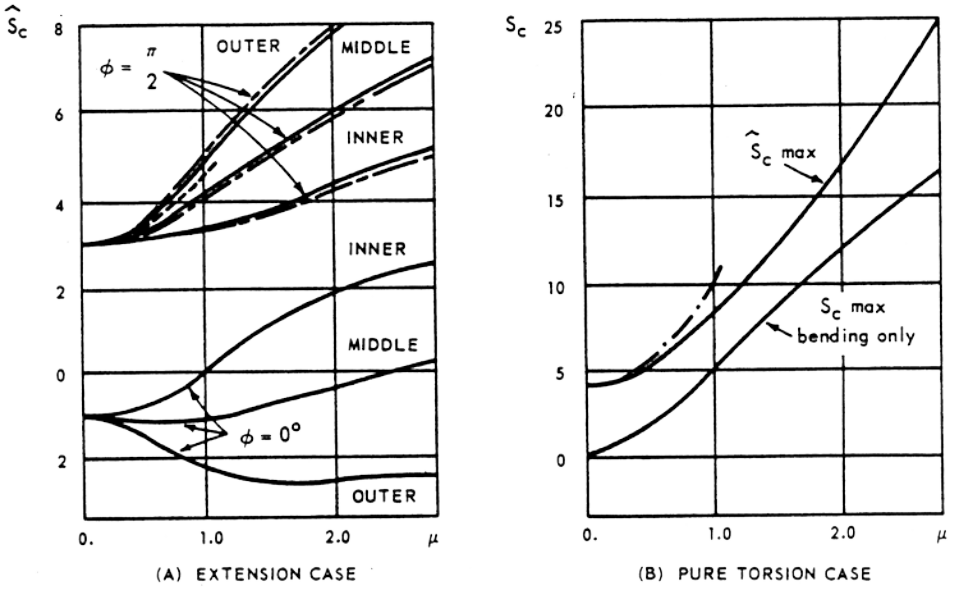

(A) EXTENSION CASE

(B) PURE TORSION CASE

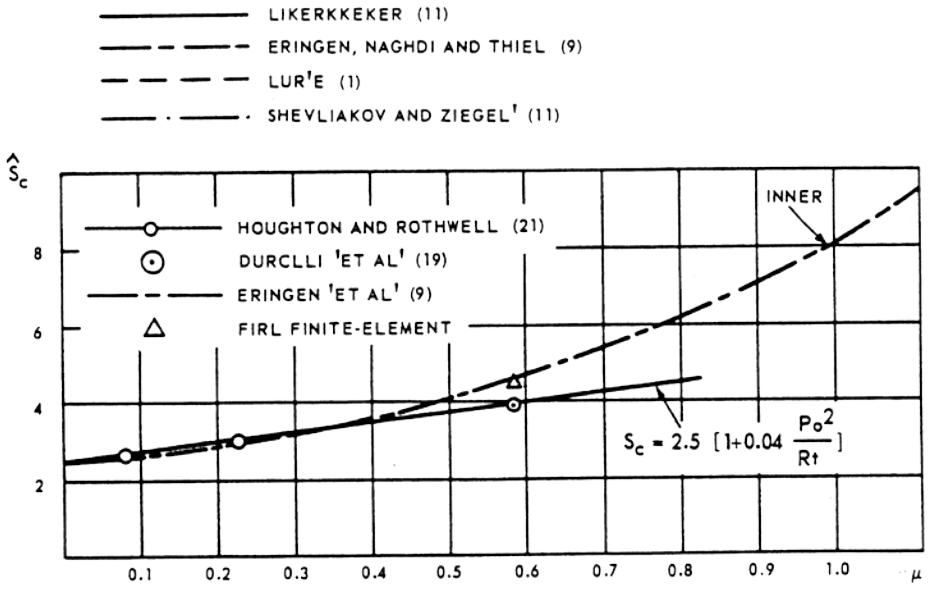

(C) CAPPED CYLINDER UNDER INTERNAL PRESSURE

GILBERT ASSOCIATES, INC.

FIGURE 3

Figure 4

GRID FOR FINITE ELEMENT ANALYSIS
OF THE STRESSES AROUND OPENINGS

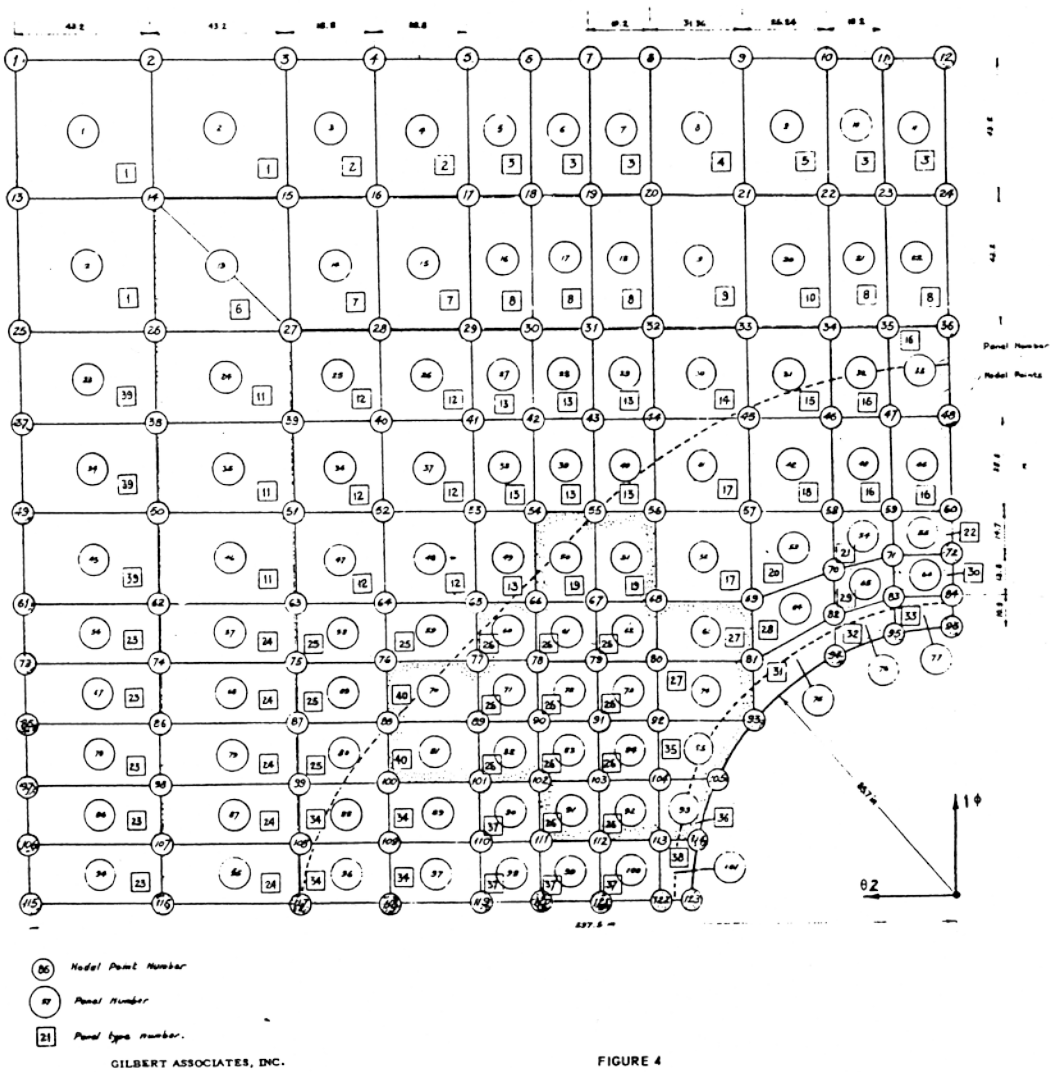

GILBERT ASSOCIATES, INC.

FIGURE 4

Figure 5

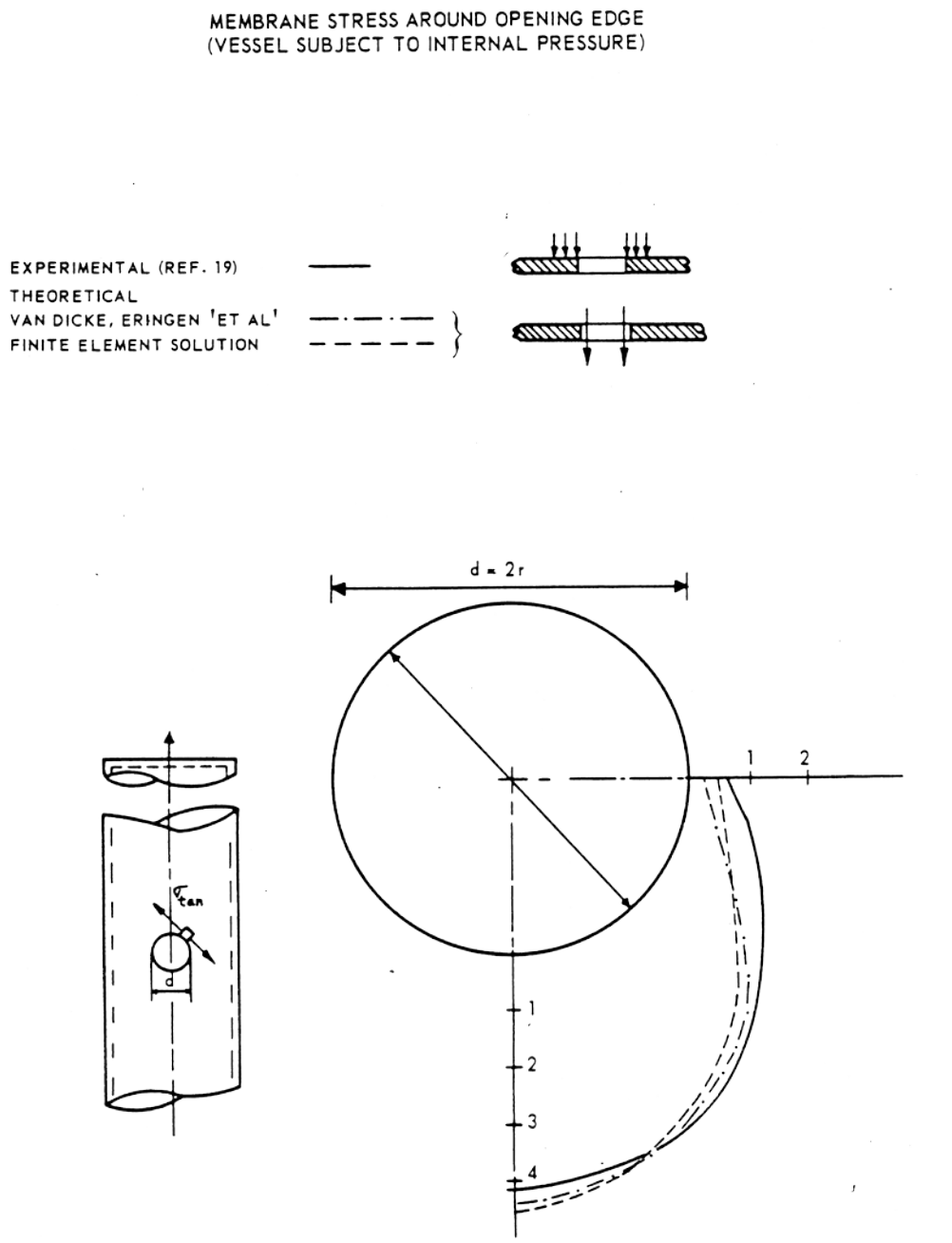
MEMBRANE STRESS AROUND OPENING EDGE
(VESSEL SUBJECT TO INTERNAL PRESSURE)
EXPERIMENTAL (REF. 19)
THEORETICAL
VAN DICKE, ERINGEN 'ET AL'
FINITE ELEMENT SOLUTION
d = 2r
1
2
1
2
3
4
GILBERT ASSOCIATES, INC.
FIGURE 5

Figure 6

SURFACE STRESSES AROUND-OPENING EDGE
(VESSEL SUBJECT TO INTERNAL PRESSURE)

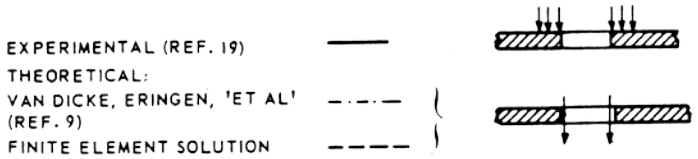

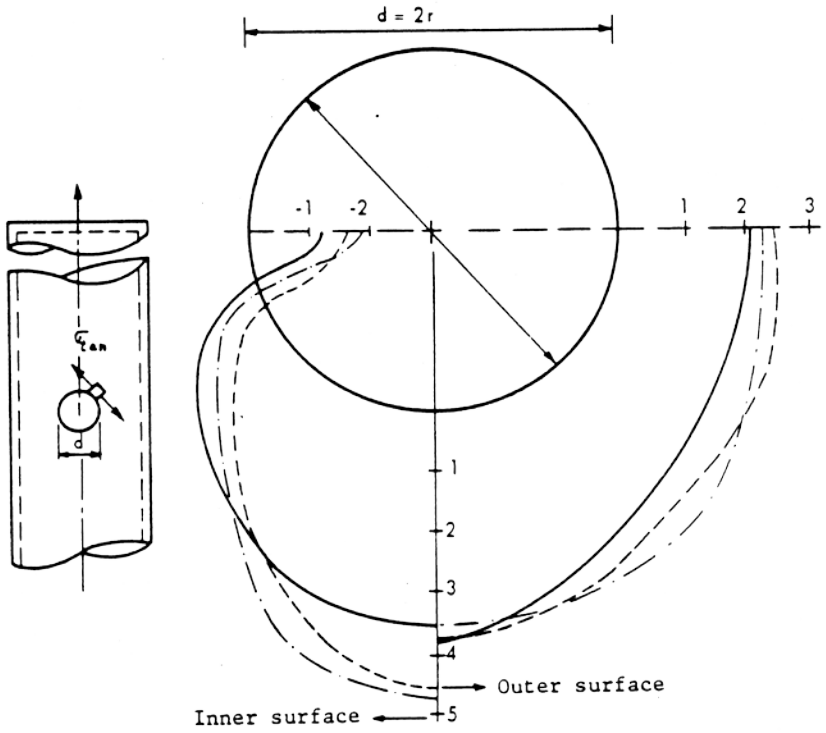

GILBERT ASSOCIATES, INC.

FIGURE 6

Figure 7

HOOP STRESSES ALONG LONGITUDINAL AXIS
(VESSEL SUBJECT TO INTERNAL PRESSURE)

EXPERIMENTAL (REF. 19) PHOTOELASTICITY ——————
HUGGENBERGER TENSOMETER o
FINITE ELEMENT SOLUTION – – – – – – –

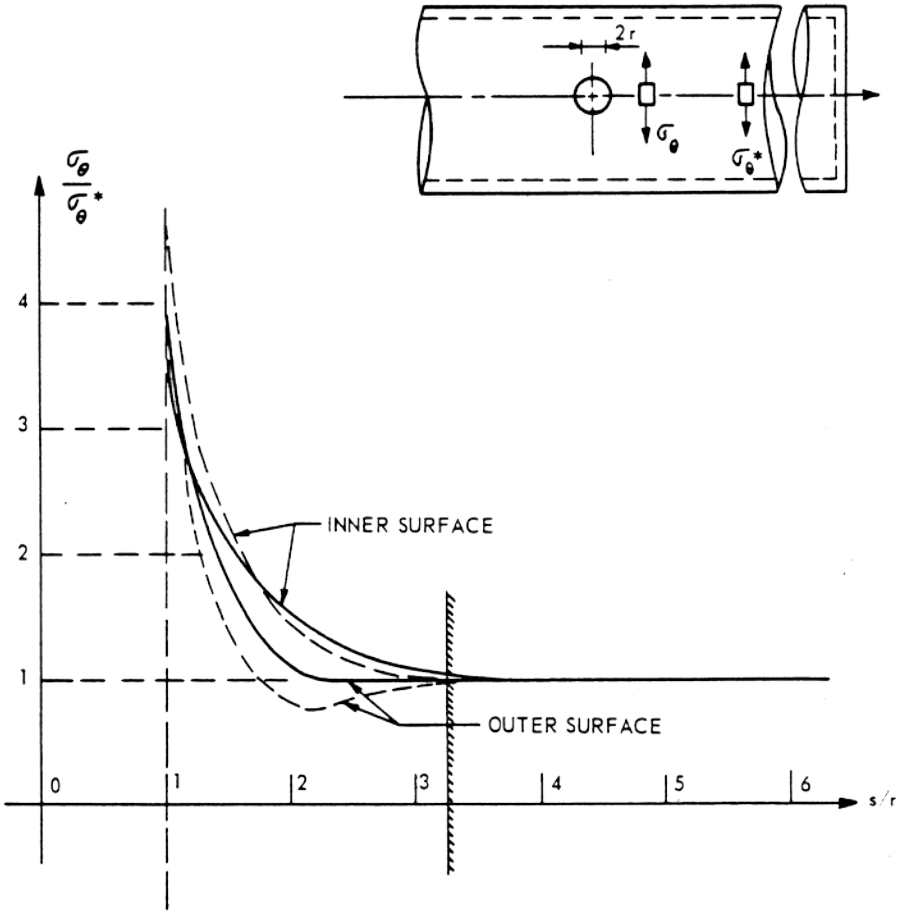

GILBERT ASSOCIATES, INC.

FIGURE 7

Figure 8

AXIAL STRESSES ALONG TRANSVERSE AXIS
(VESSEL SUBJECT TO INTERNAL PRESSURE)

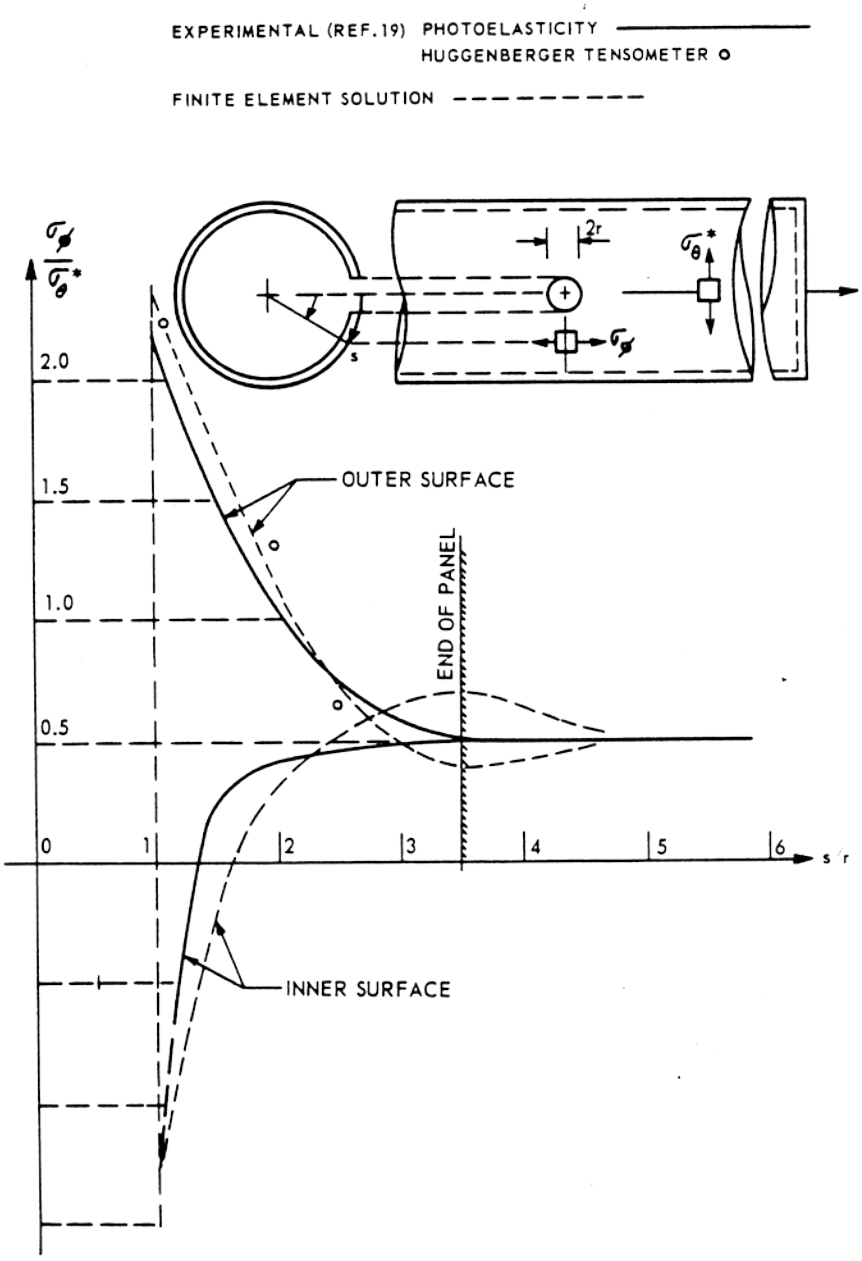

GILBERT ASSOCIATES, INC.

FIGURE 8

Figure 9

HOOP STRESS-RESULTANT N_θ ALONG SYMMETRY AXES
(TEST PROBLEM)

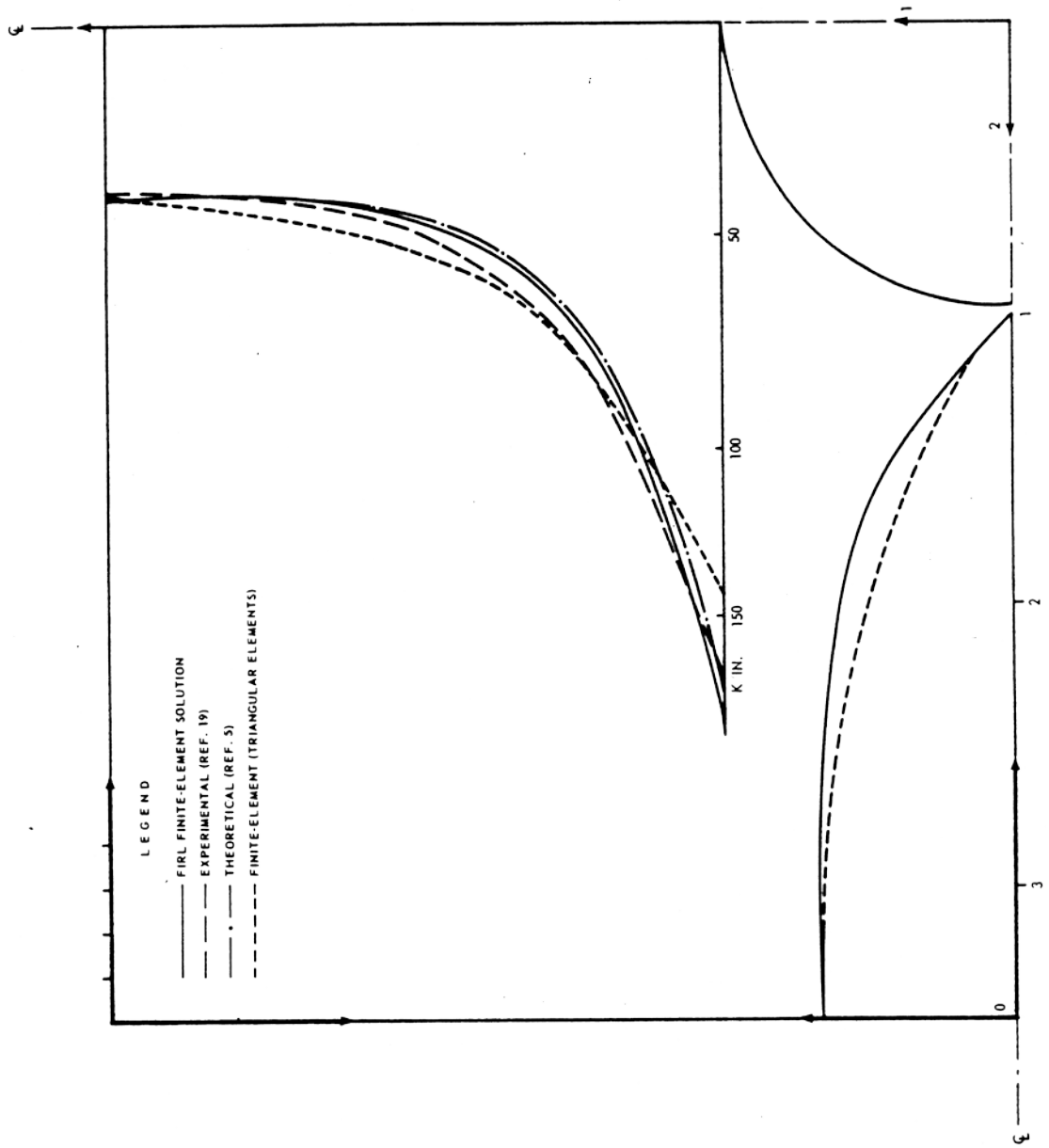

GILBERT ASSOCIATES, INC.

FIGURE 9

Figure 10

LAYER THICKNESSES AND DESIGNATION

TYPICAL SHELL

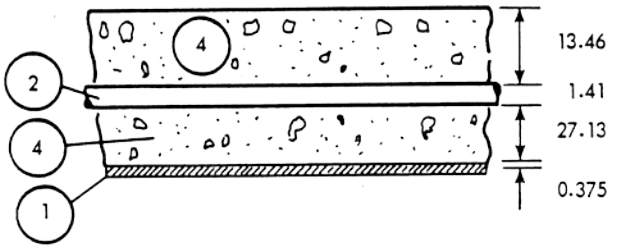

REINFORCED SHELL

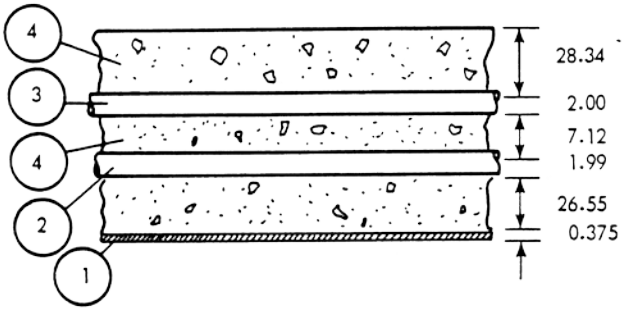

GILBERT ASSOCIATES, INC.

FIGURE 10

Figure 11

NODAL FORCES DUE TO CURVATURE OF TENDONS IN NEIGHBORHOOD OF OPENING

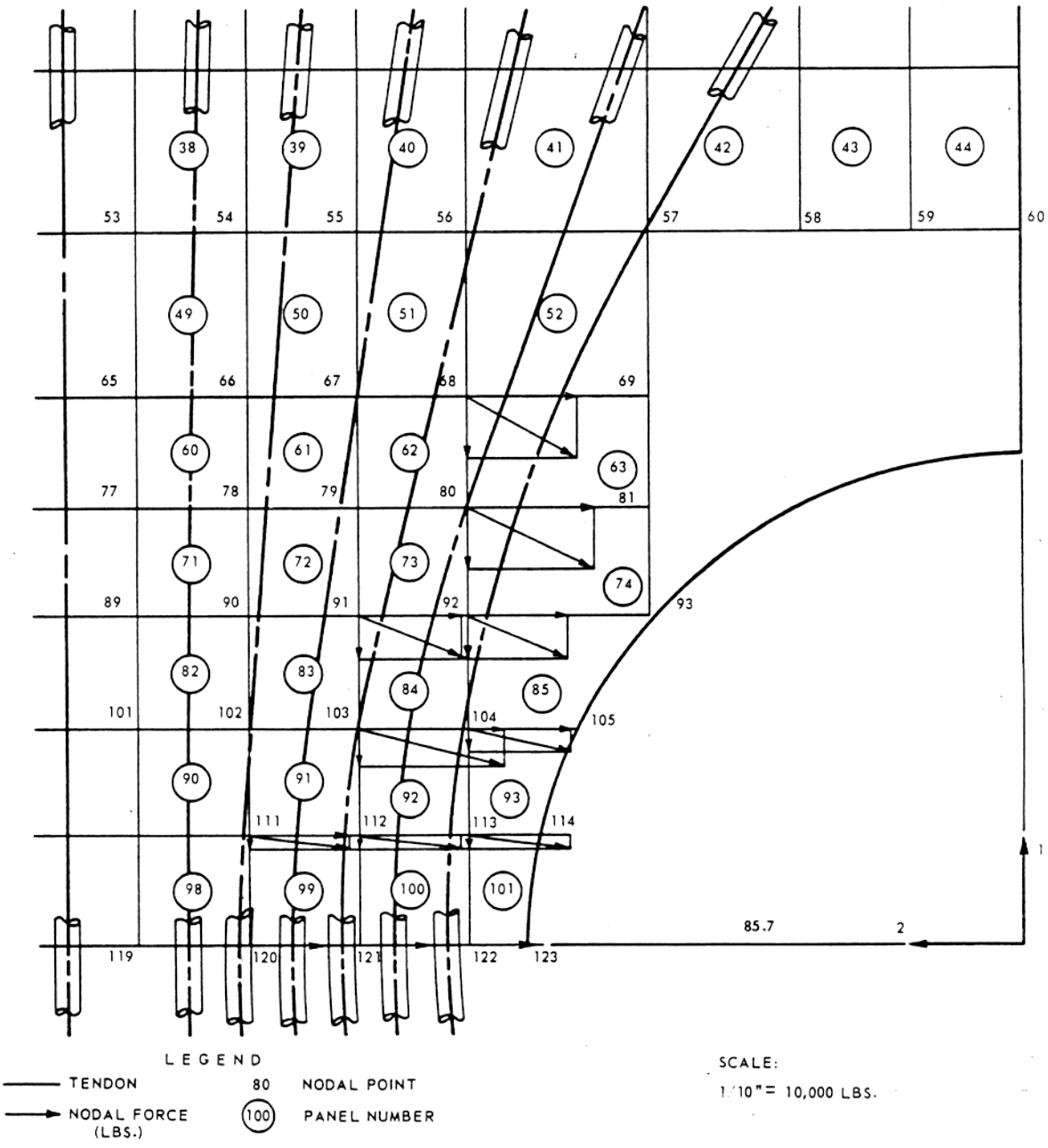

GILBERT ASSOCIATES, INC.

FIGURE 11

Figure 12

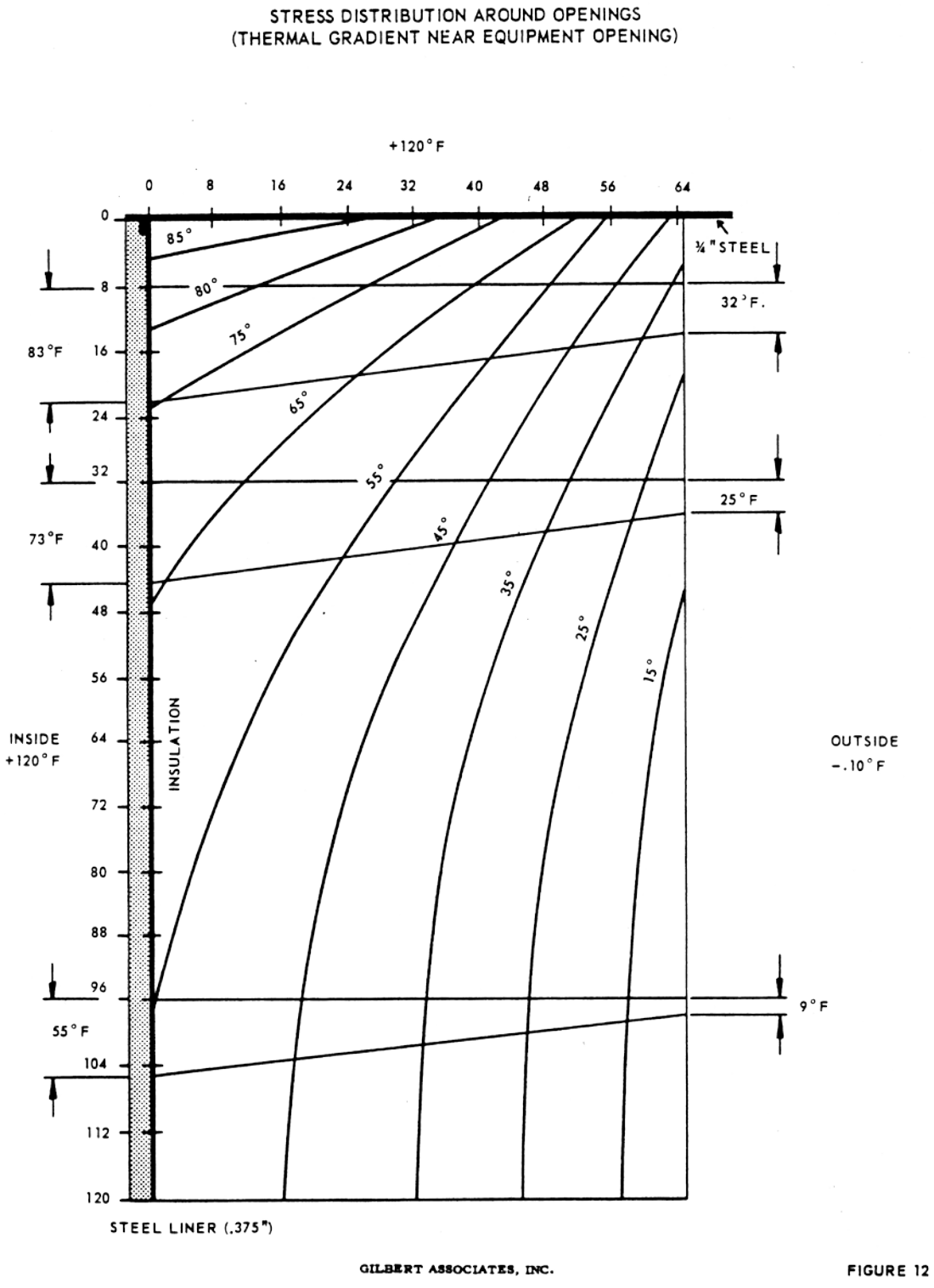

FIGURE 12

Figure 13 Steady State Temperature Distributions - Winter Gradient

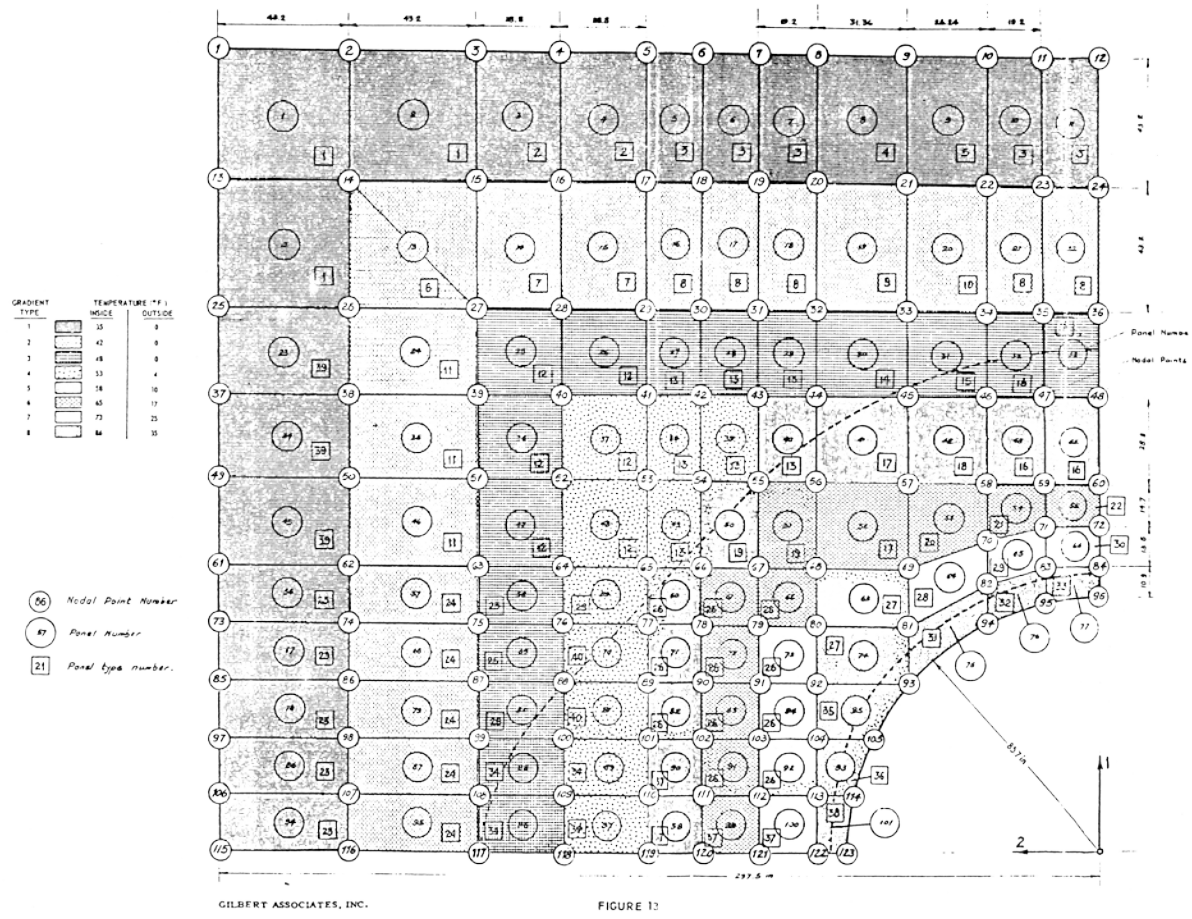

Figure 14

STRESS DISTRIBUTION AROUND OPENINGS
(EFFECT OF BOND FAILURE ALONG TERMINATED REBARS)

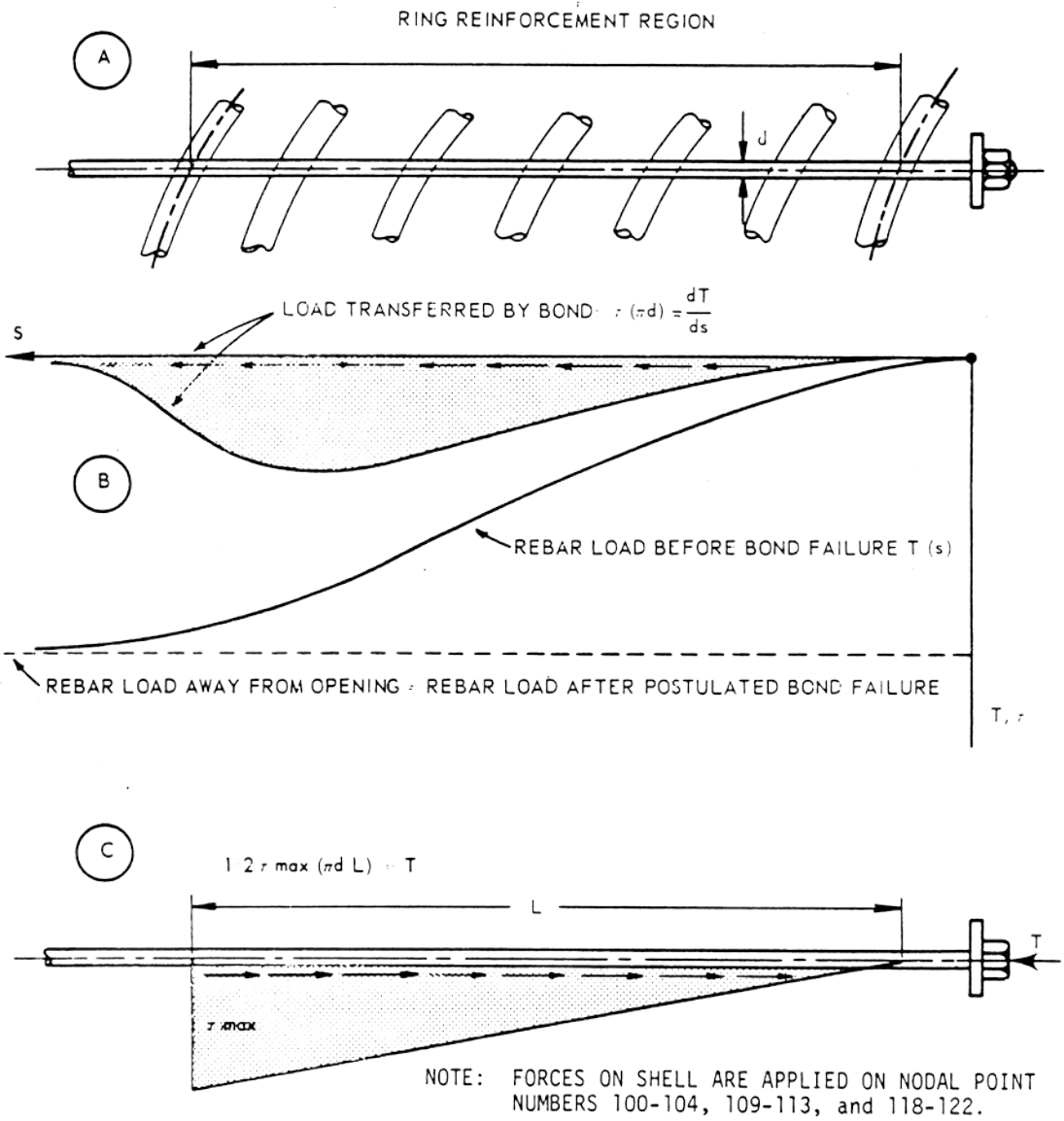

LOADS APPLIED IN FINITE ELEMENT ANALYSIS

GILBERT ASSOCIATES, INC. FIGURE 14

Figure 15

HOOP STRESS RESULTANTS ALONG HORIZONTAL AND VERTICAL SYMMETRY AXES
(INTERNAL PRESSURE = 69 PSI

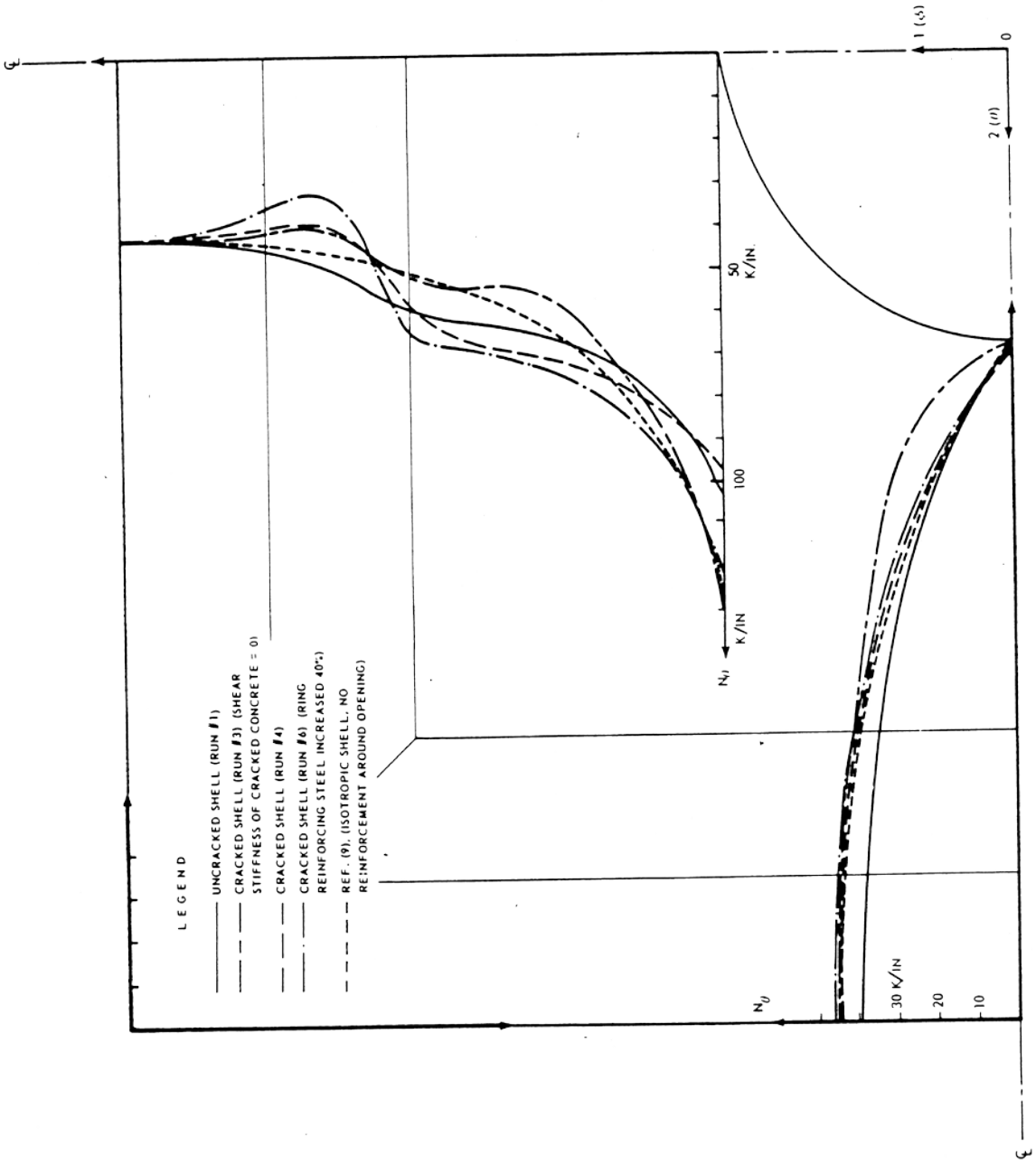

GILBERT ASSOCIATES, INC.

FIGURE 15

Figure 16

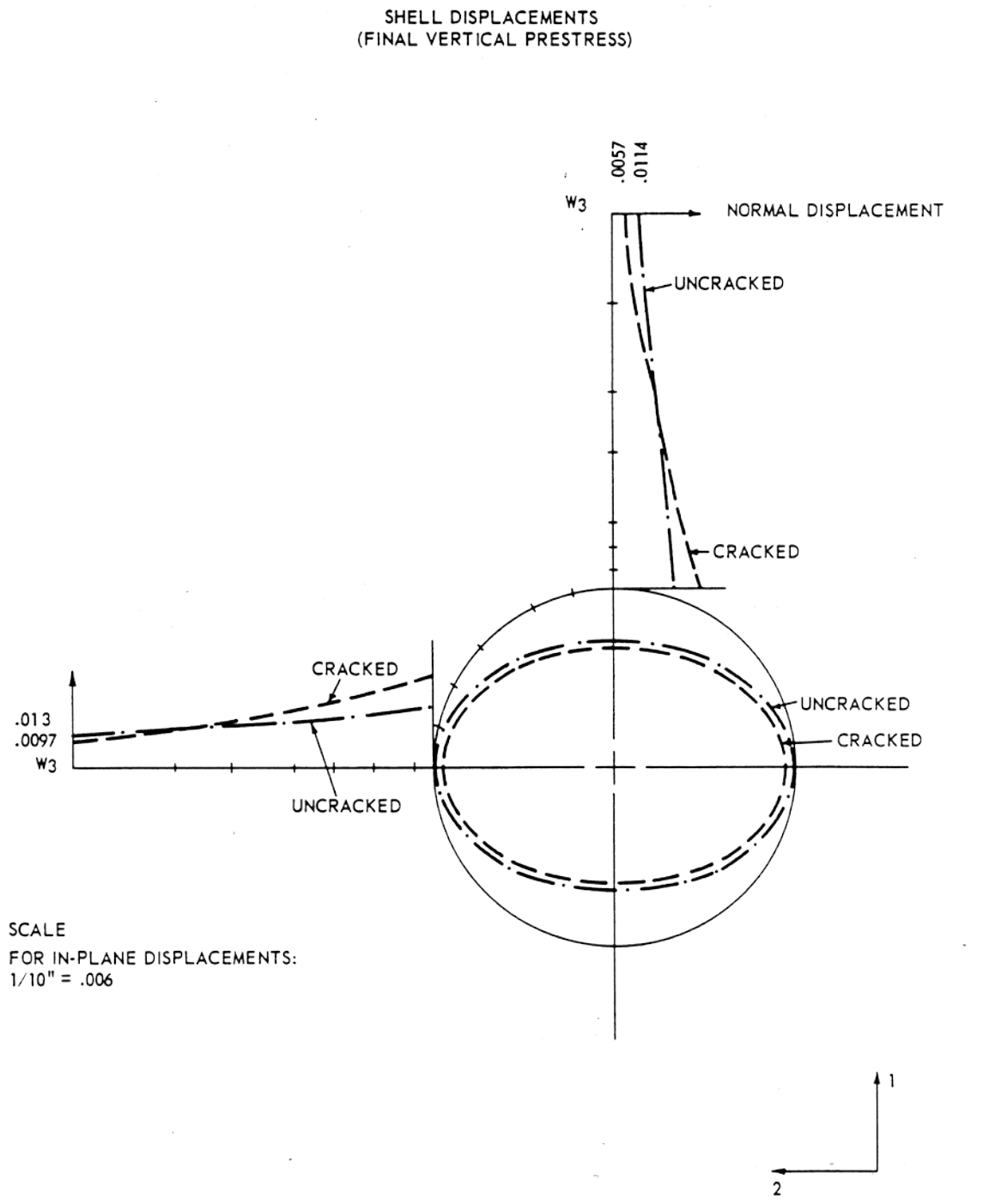
SHELL DISPLACEMENTS
(FINAL VERTICAL PRESTRESS)
.0057
.0114
W3
NORMAL DISPLACEMENT
UNCRACKED
CRACKED
CRACKED
UNCRACKED
.013
.0097
W3
UNCRACKED
UNCRACKED
CRACKED
SCALE
FOR IN-PLANE DISPLACEMENTS:
1/10" = .006
1
2
GILBERT ASSOCIATES, INC.
FIGURE 16

Figure 17

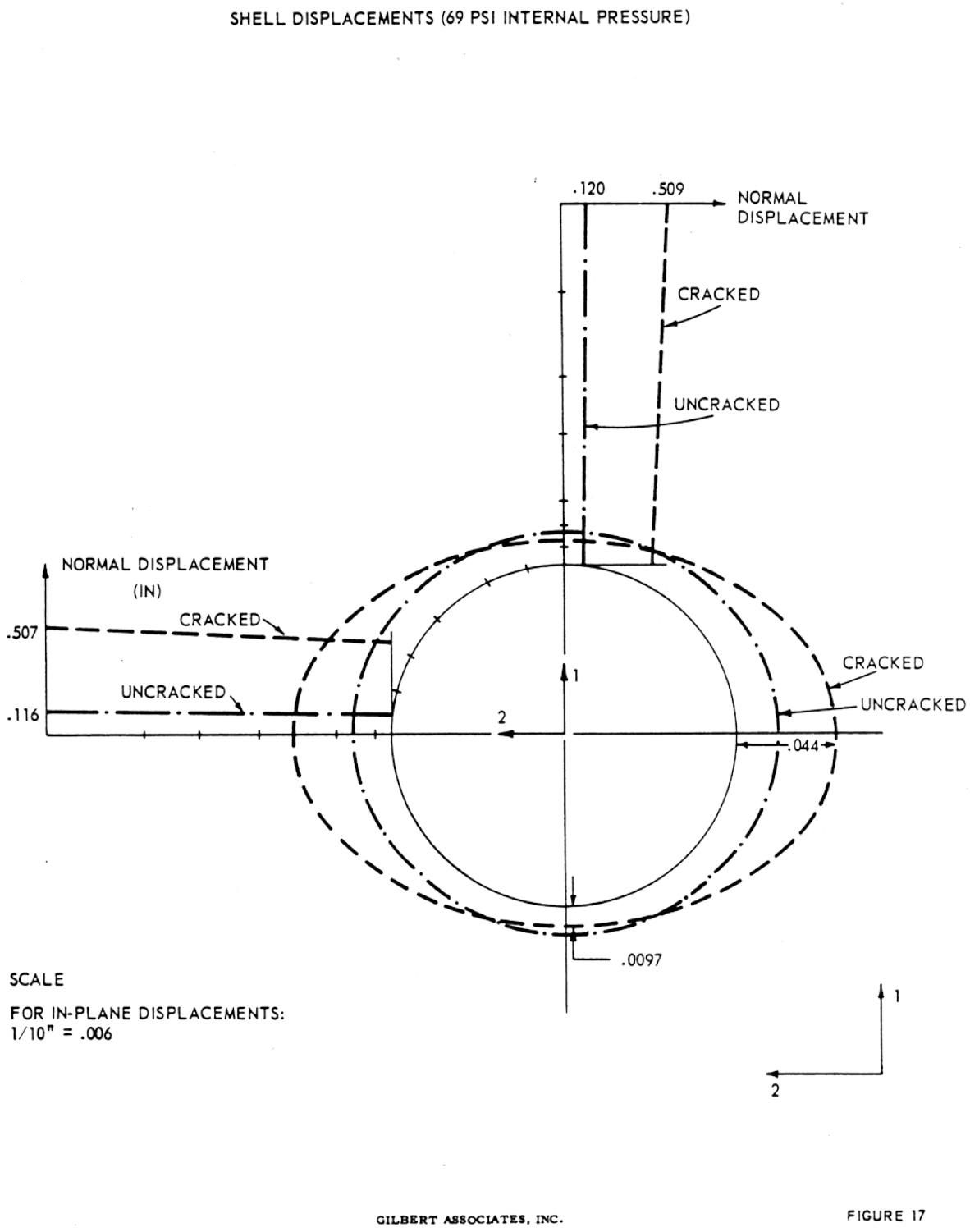
SHELL DISPLACEMENTS (69 PSI INTERNAL PRESSURE)
.120
.509
NORMAL DISPLACEMENT
CRACKED
UNCRACKED
NORMAL DISPLACEMENT (IN)
.507
CRACKED
.116
UNCRACKED
1
2
CRACKED
UNCRACKED
.044
.0097
SCALE
FOR IN-PLANE DISPLACEMENTS:
1/10" = .006
1
2
GILBERT ASSOCIATES, INC.
FIGURE 17

Figure 18

INTERACTION DIAGRAM FOR AXIAL
COMPRESSION/TENSION AND BENDING

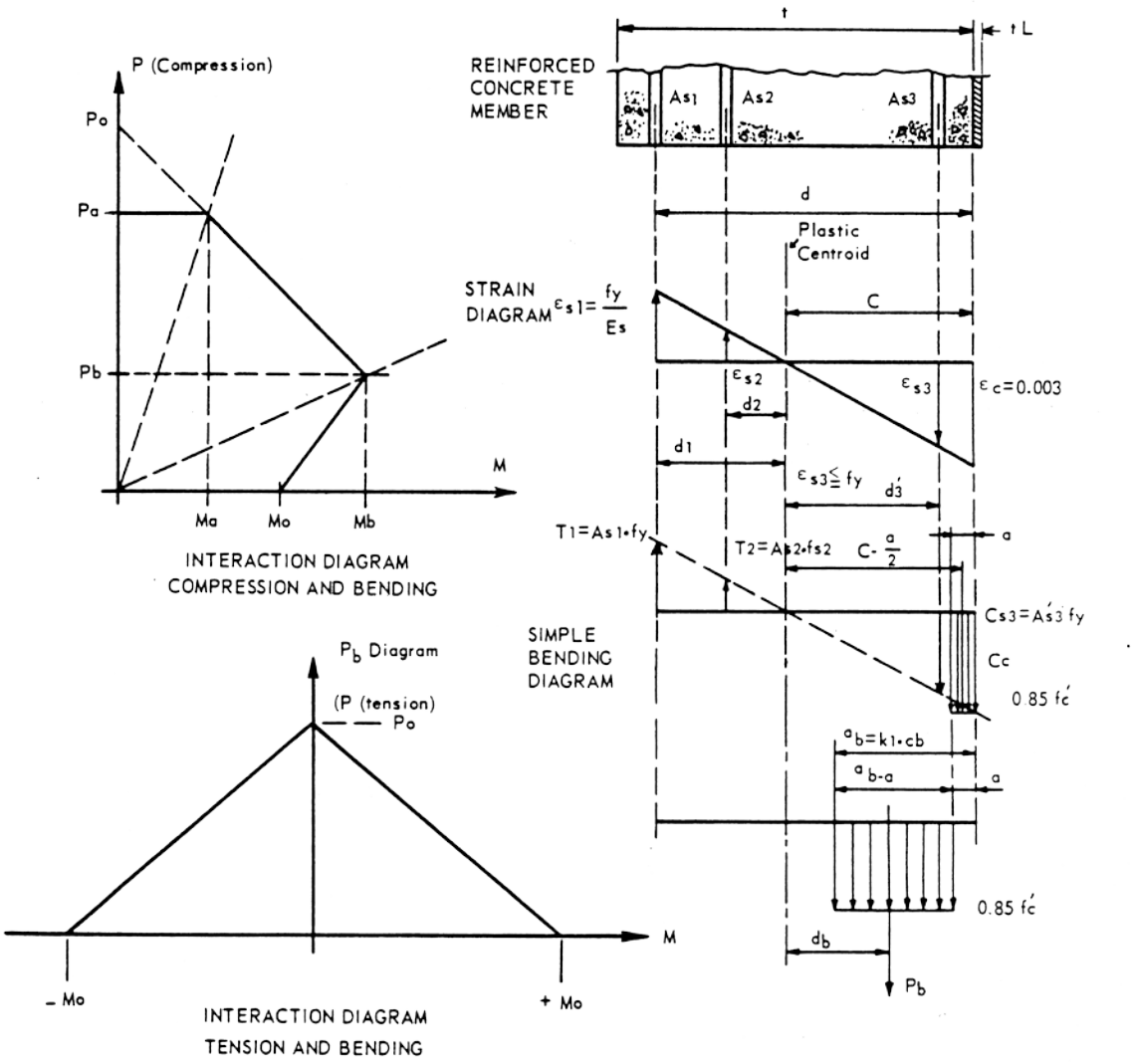

GILBERT ASSOCIATES, INC. FIGURE 18

Figure 19

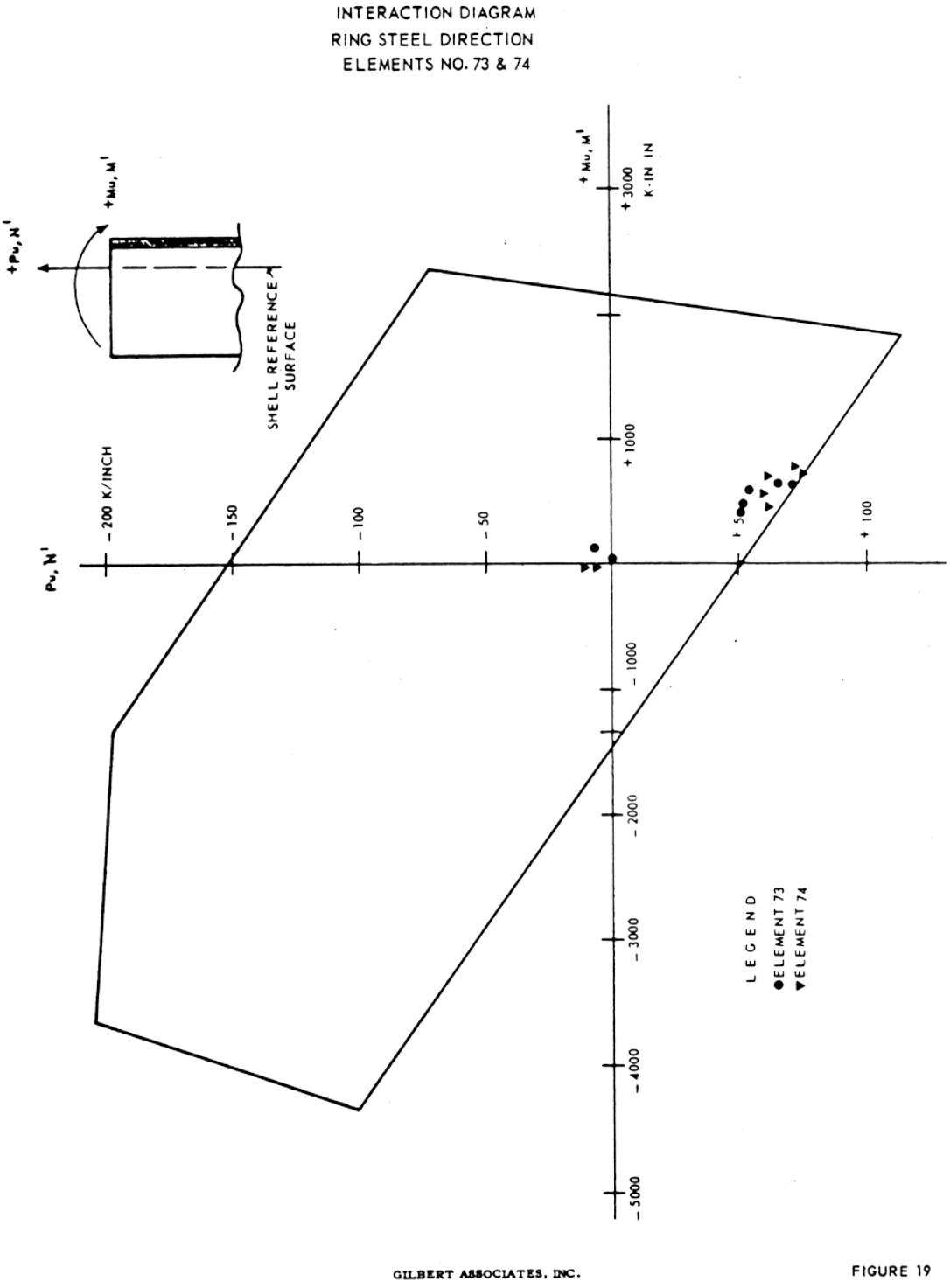

GILBERT ASSOCIATES, INC.

FIGURE 19

Figure 20

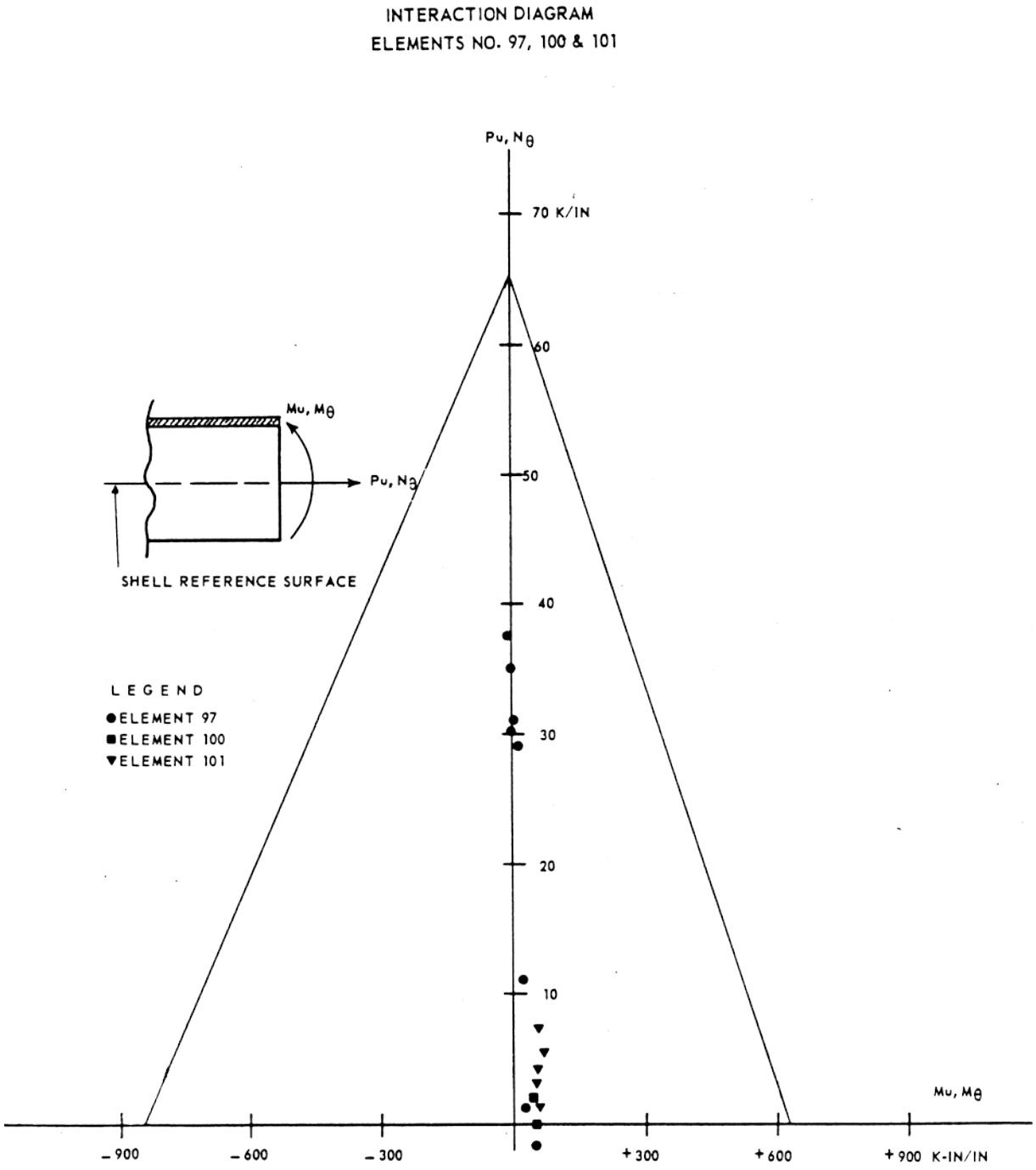

GILBERT ASSOCIATES, INC.

FIGURE 20

Figure 21

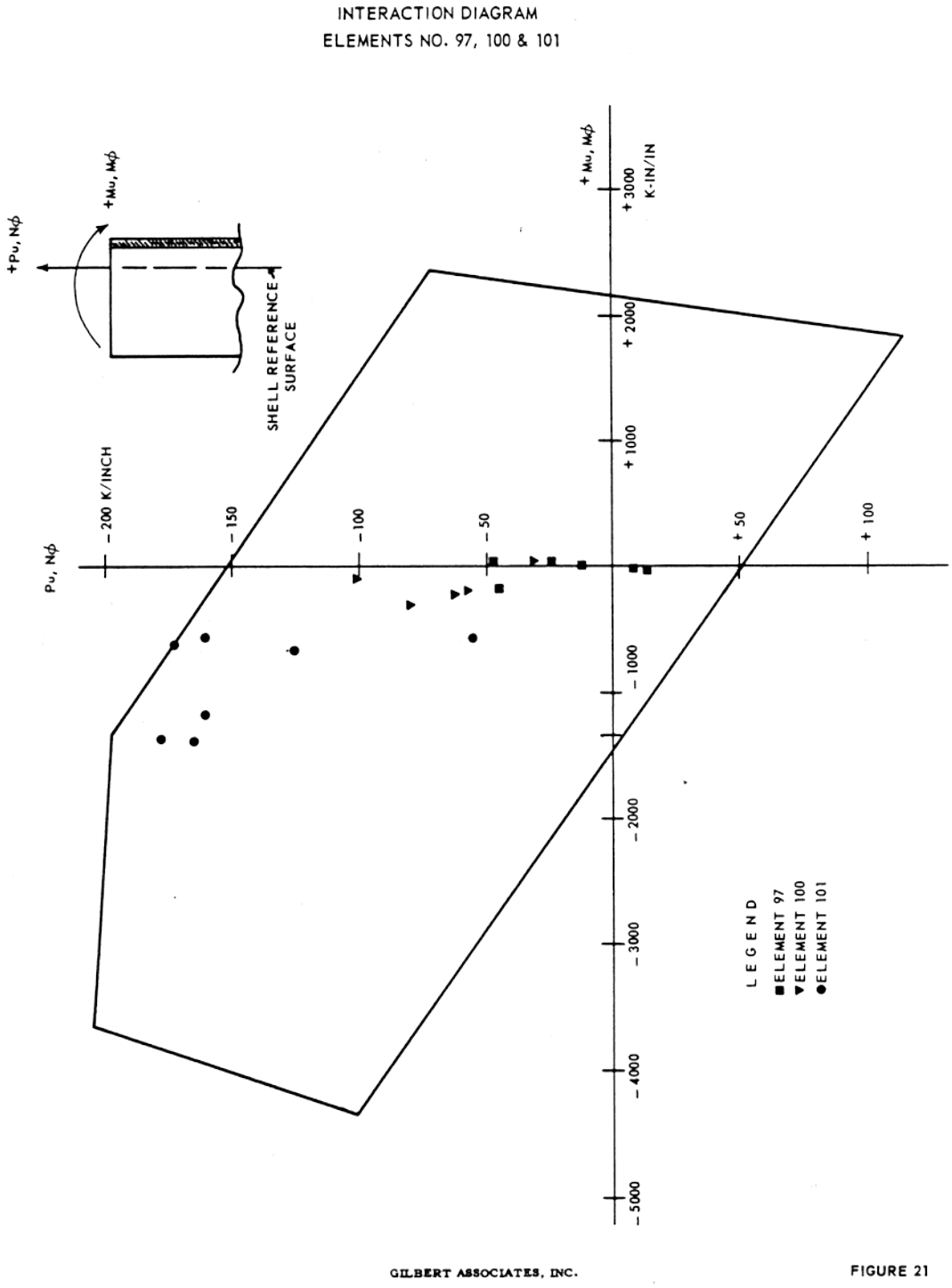
INTERACTION DIAGRAM
ELEMENTS NO. 97, 100 & 101
+Pu, Nφ
+Mu, Mφ
SHELL REFERENCE SURFACE
+ Mu, Mφ
K-IN/IN
+ 3000
+ 2000
+ 1000
- 1000
- 2000
- 3000
- 4000
- 5000
Pu, Nφ
- 200 K/INCH
- 150
- 100
- 50
+ 50
+ 100
LEGEND
■ELEMENT 97
▼ELEMENT 100
●ELEMENT 101
GILBERT ASSOCIATES, INC.
FIGURE 21

Figure 22

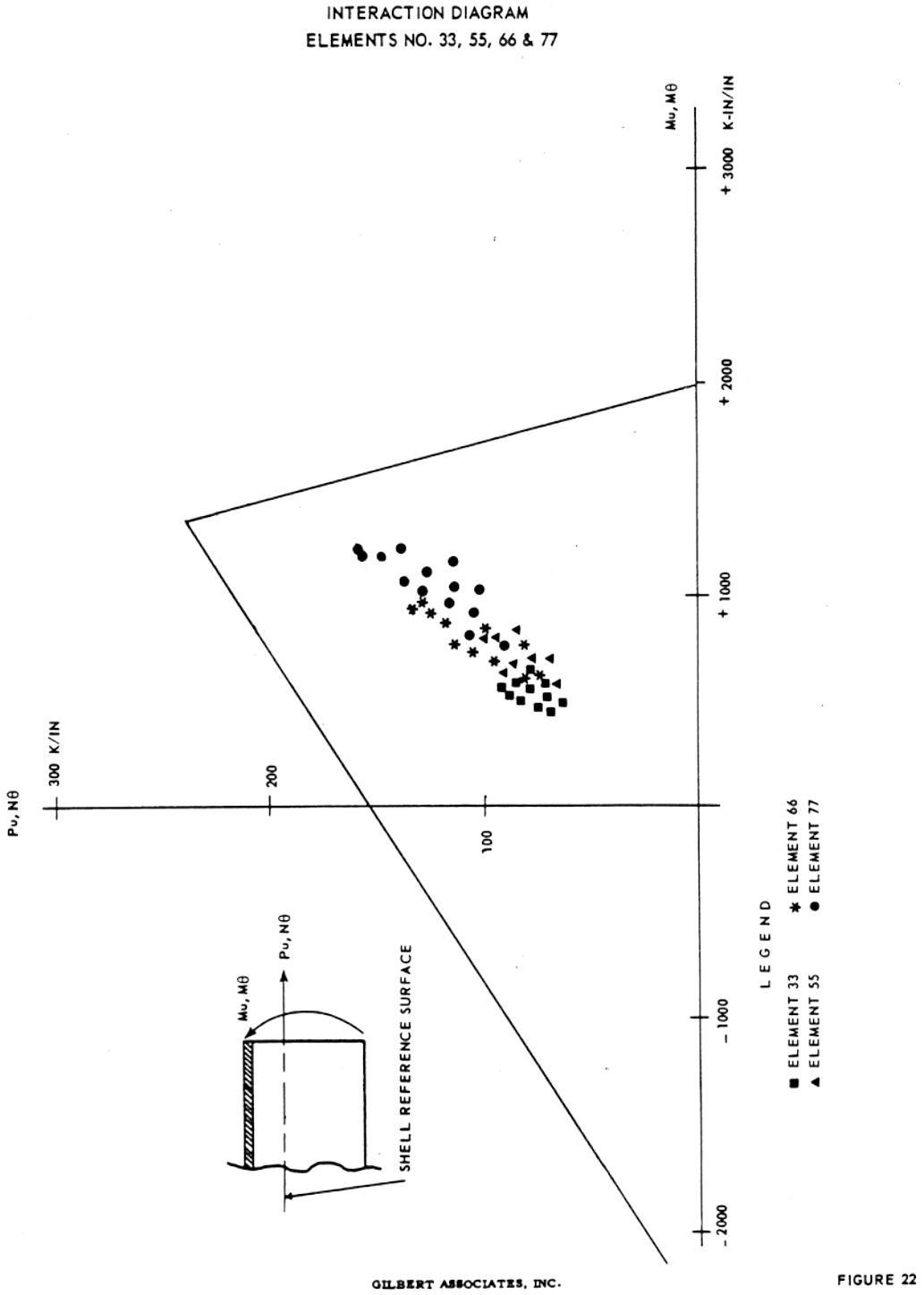

FIGURE 22

Figure 23

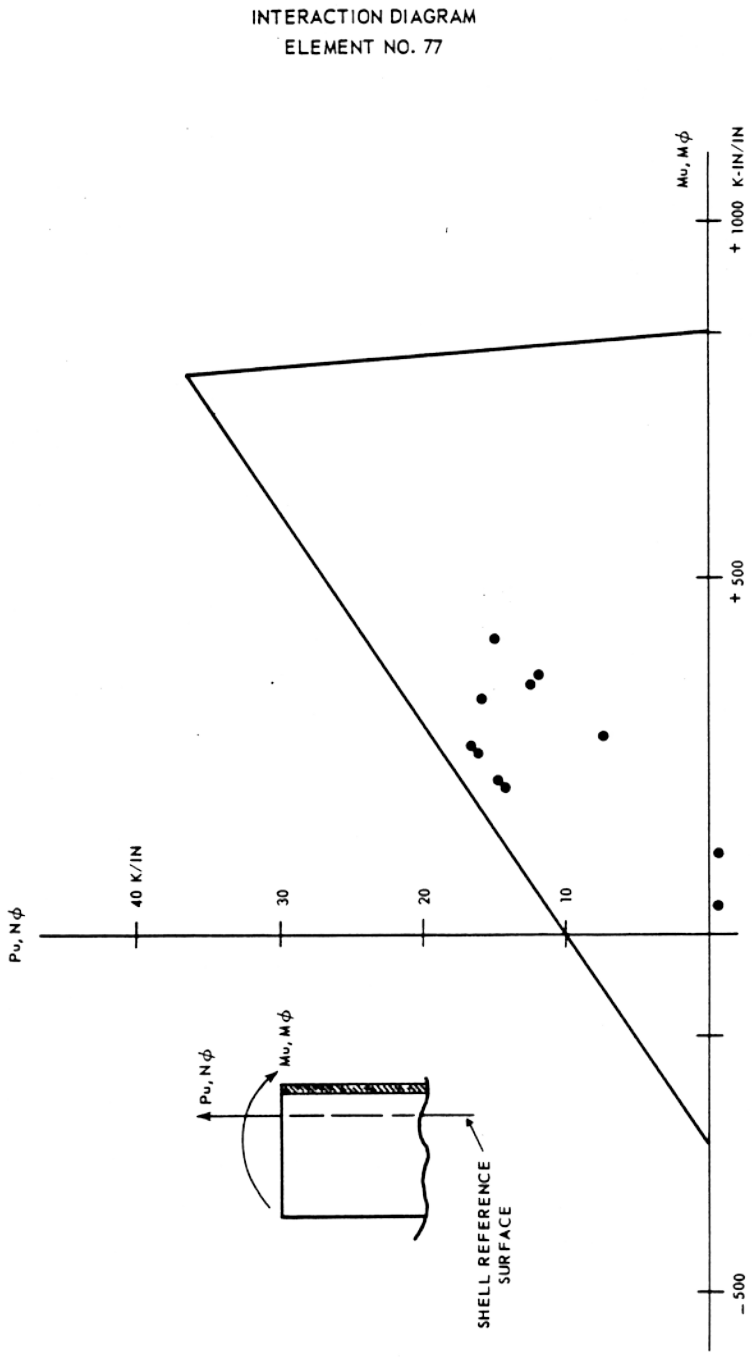

FIGURE 23

Figure 24

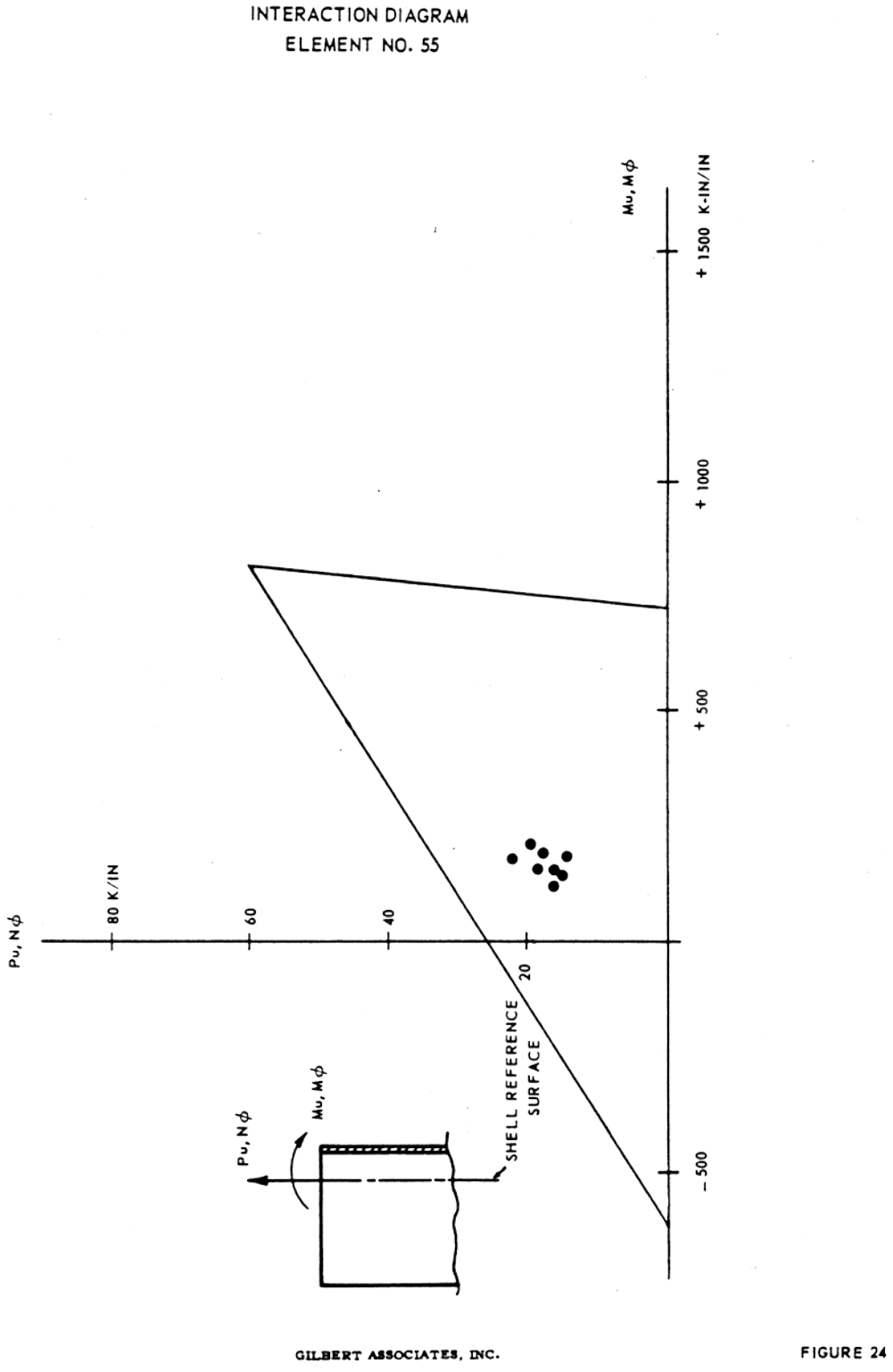
INTERACTION DIAGRAM
ELEMENT NO. 55
Mu, Mϕ
+ 1500 K-IN/IN
+ 1000
+ 500
- 500
Pu, Nϕ
80 K/IN
60
40
20
SHELL REFERENCE SURFACE
Pu, Nϕ
Mu, Mϕ
GILBERT ASSOCIATES, INC.
FIGURE 24

Drawings

APPENDIX 3B

D R A W I N G S

Figure Drawing 1Reactor Containment Vessel - Equipment/Personnel Access Reinforcement - Enlarged Sections

Figure Deleted

Refer to Drawing
D421-0024 Rev. 006

Figure Drawing 2Reactor Containment Vessel - Equipment Access Opening Reinforcement - Stretch-out & Sections

Figure Deleted

Refer to Drawing
D421-0022 Rev. 007

Figure I *Comparison of H.H. & GAI Results Hoop Stress Resultants Along Horizontal and Vertical Symmetry Axes (Internal Pressure = 69 PSI)*

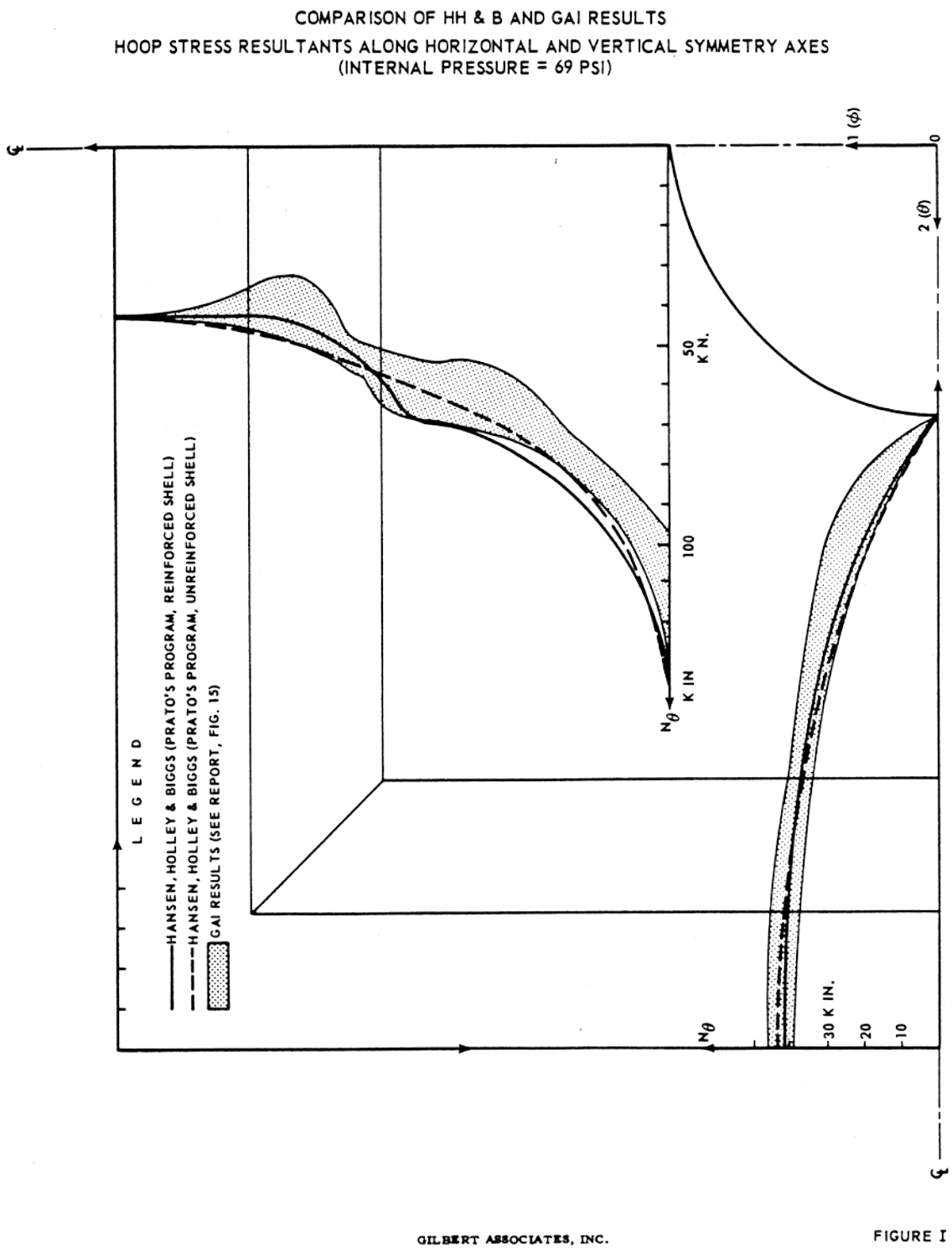

Figure Drawing 1Reactor Containment Vessel - Equipment/Personnel Access Reinforcement - Enlarged Sections

Figure Deleted

Refer to Drawing
D421-0024 Rev. 006

Figure Drawing 2Reactor Containment Vessel - Equipment Access Opening Reinforcement - Stretch-out & Sections

Figure Deleted

Refer to Drawing
D421-0022 Rev. 007

Figure Drawing 3 Large Openings - Pour Schedule

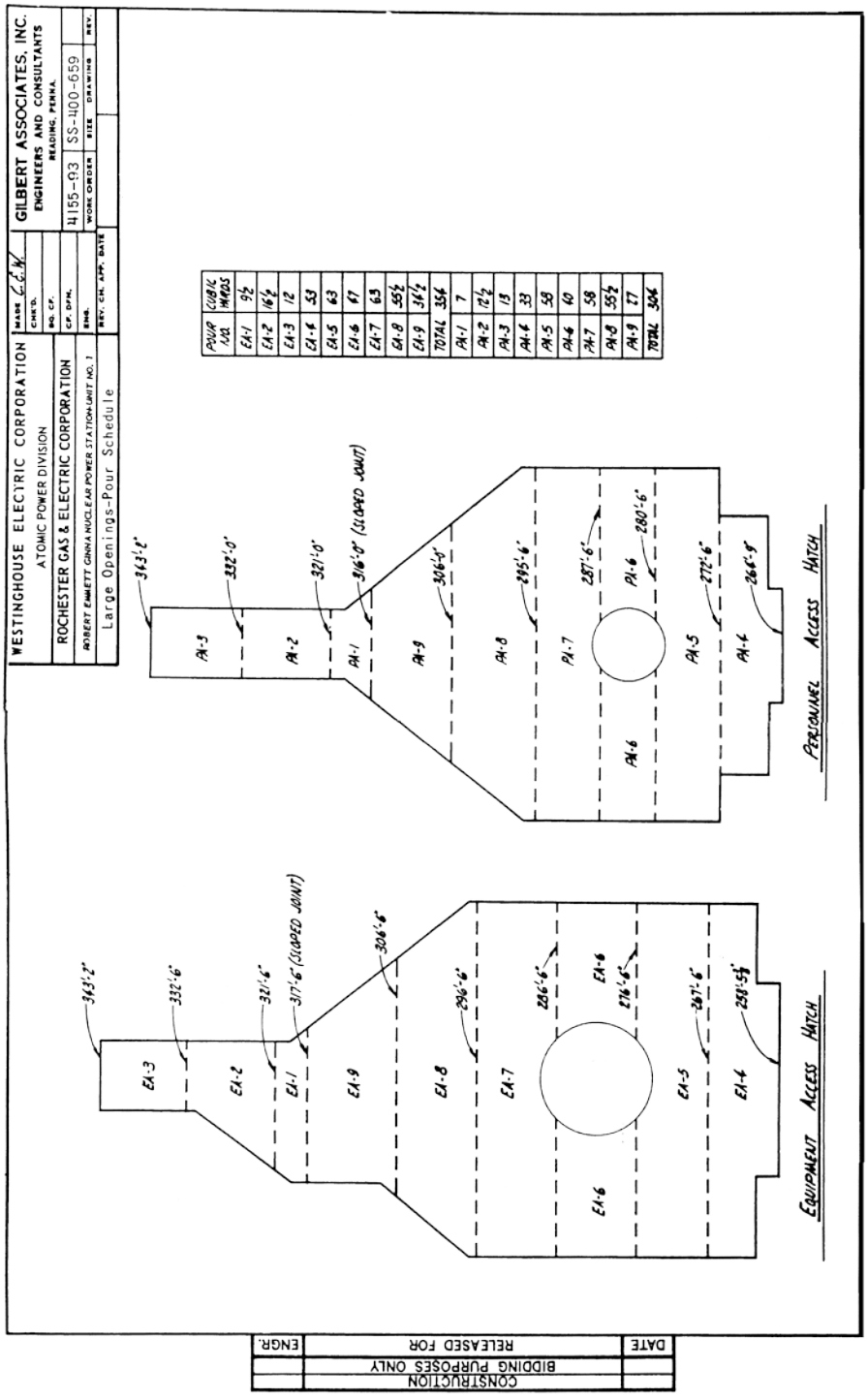

POUR NO.	CUBIC YARDS
EA-1	9½
EA-2	16½
EA-3	12
EA-4	53
EA-5	63
EA-6	67
EA-7	63
EA-8	55½
EA-9	34½
TOTAL	364
PA-1	7
PA-2	12½
PA-3	13
PA-4	33
PA-5	58
PA-6	40
PA-7	58
PA-8	55½
PA-9	17
TOTAL	304